Pulsed Nuclear Magnetic Resonance

Rico Schmidt and Guido Falk von Rudorff

This experiment deals with the theoretical background of the analysis through NMR. This method is used for non-invasive diagnostic of a medical investigation as well as for conformation and geometry analysis in material sciences, chemistry or physics.

I Introduction

Each proton has nuclear spin $\mathbf{I}$ with $|\mathbf{I}| = \sqrt{I(I+1)}\hbar$– just like all angular momentum related quantum numbers. The z component of $\mathbf{I}$ is given by

$$M_I = -I, -I+1, \ldots, I \tag{1}$$

For protons (which are in fact fermions), the quantum number is known[1] to be $I = \frac{1}{2}$ so $M_I = -\frac{1}{2}, \frac{1}{2}$. The selection rule is $\Delta M_I = \pm 1$. For the magnetic moment, we have

$$\boldsymbol{\mu}_I = g_K \mu_K \mathbf{I} = \gamma_I \hbar \mathbf{I} \tag{2}$$

with the gyromagnetic relationship γ_I and

$$\mu_K = \frac{e}{2m_p}\hbar \tag{3}$$

Under the influence of an external magnetic field $\mathbf{B_0} = B_0 \hat{e}_z$, this magnetic moments separates the degenerate states at E_0

$$E(M_I) = E_0 - \gamma_I \hbar B_0 M_I \tag{4}$$

In general, the sign only affects the order of the energy levels according to eqn. (1). The selection rule mentioned before leads to the conclusion, that all transitions share the same energy difference

$$\begin{aligned}\Delta E &= |E(M_I) - E(M_I')| = \gamma_I \hbar B_0 |M_I - M_I'| \\ &= \gamma_I \hbar B_0 \end{aligned} \tag{5}$$

In order to induce transitions, the resonance frequency f_r has to be found

$$h f_r = \Delta E \Leftrightarrow f_r = \frac{\gamma_I}{2\pi} B_0 \tag{6}$$

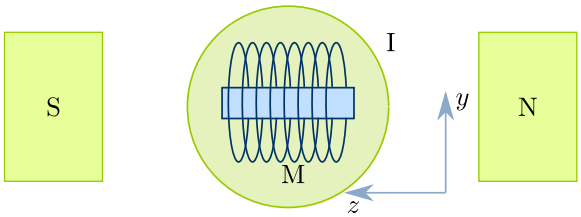

Figure 1. Experimental setup with induction coil I and measurement coil M.

I.A Bloch equations

As this experiment is not able to operate on single protons, we have to find mathematical methods in order to deal with the total magnetic momentum $\mathbf{M_0}$ formed by the addition of all the protons' spins. Any analyzed material can be expected[2] to contain at least some 10^{17} spins, so statistical effects are neglectable. For $\mathbf{M_0}$, the influence of the external magnetic field can be described[2] using

$$\frac{\mathrm{d}}{\mathrm{d}t}\mathbf{M} = \gamma_I \mathbf{M} \times \mathbf{B}_0 \tag{7}$$

For an external magnetic field, $\mathbf{M_0}$ is given[3] by the static magnetic susceptibility χ_0

$$\mathbf{M_0} = \chi_0 \mathbf{B_0} = \frac{N g_K^2 \boldsymbol{\mu}_K^2 I(I+1)}{3 k_B T}\mathbf{B_0} \tag{8}$$

with the number of nuclear spins per volume N.

The magnetic momentum M_0 precesses around the axis of the external magnetic field with the frequency[2]

$$\omega_L = \gamma_I B_0 \tag{9}$$

which is identical to the resonance frequency f_r and is called Larmor frequency. In the following, the observer is placed in a reference system rotating around $\hat{\mathbf{e}}_z$ with ω_L[4]. Adding the effects of relaxation described later on, we obtain[3] the Bloch equations

$$\frac{\mathrm{d}\mathbf{M_0}\hat{\mathbf{e}}_x}{\mathrm{d}t} = \omega_L \mathbf{M_0}\hat{\mathbf{e}}_y - \frac{\mathbf{M_0}\hat{\mathbf{e}}_\mathbf{x}}{T_2} \tag{10}$$

$$\frac{\mathrm{d}\mathbf{M_0}\hat{\mathbf{e}}_y}{\mathrm{d}t} = -\omega_L \mathbf{M_0}\hat{\mathbf{e}}_x - \frac{\mathbf{M_0}\hat{\mathbf{e}}_\mathbf{y}}{T_2} \tag{11}$$

$$\frac{\mathrm{d}\mathbf{M_0}\hat{\mathbf{e}}_z}{\mathrm{d}t} = -\frac{\mathbf{M_0}\hat{\mathbf{e}}_\mathbf{z} - |\mathbf{M_0}|}{T_1} \tag{12}$$

According to eqn. (4), the $M_I^+ = \frac{1}{2}$ state is lower than the $M_I^- = -\frac{1}{2}$ one. As we assumed thermal equilibrium

Table I. Relevant constants.

symbol	value	comment
γ_I	$2.67522 \cdot 10^8$ rad s^{-1} T^{-1}	proton only
μ_B	$9.27401 \cdot 10^{-24}$ J T^{-1}	universal
μ_K	$5.05079 \cdot 10^{-27}$ J T^{-1}	universal
g_K	5.58562	proton only

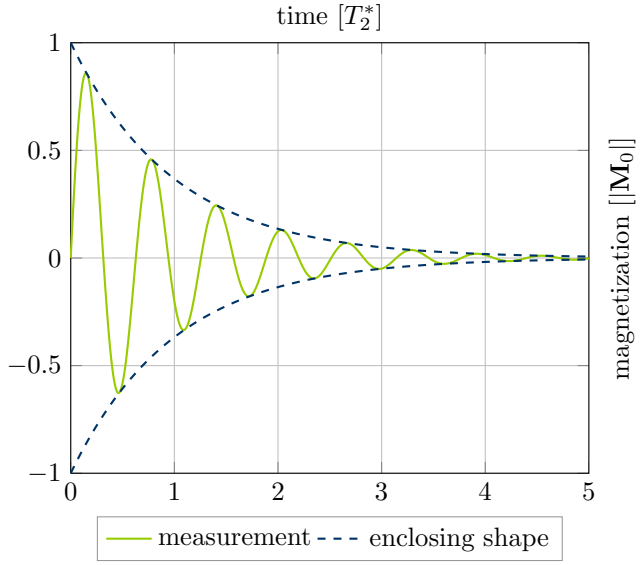

Figure 2. Free induction decay according to [4, 5] for $\omega \neq \omega_L$ (green) and $\omega = \omega_L$ (dashed blue). Theoretical values.

using a BOLTZMANN distribution, there are more protons in M_I^+ state than in M_I^- state. Thus, $\mathbf{M_0}\hat{\mathbf{e}}_z > 0$. Due to the precession, the expectation values for $\mathbf{M_0}\hat{\mathbf{e}}_x$ and $\mathbf{M_0}\hat{\mathbf{e}}_y$ are zero. However, the difference in the occupation number $N_\pm$ is quite small.

$$N_\pm = N_0 \exp\left(-\frac{E_0 \mp \frac{1}{2}\Delta E}{k_B T}\right) \tag{13}$$

For the relative difference, this relation yields

$$\begin{aligned}\frac{N_+}{N_-} &= \exp\left(-\frac{E_0 - \frac{1}{2}\Delta E}{k_B T} - \frac{E_0 + \frac{1}{2}\Delta E}{k_B T}\right) \\ &= \exp\left(\frac{\Delta E}{k_B T}\right) = \exp\left(\frac{\gamma_I \hbar B_0}{k_B T}\right)\end{aligned} \tag{14}$$

With $\gamma_I \hbar / k_B \simeq 1.28449 \cdot 10^{-2}\,\mathrm{K\,T^{-1}}$ and a low temperature environment, very strong magnetic fields are necessary in order to achieve big differences in the occupation number. As earth's magnetic field is very weak, the difference of N_+ and N_- is almost zero and the occupation numbers are almost identical. Therefore, when placing the sample within the magnetic field $\mathbf{B}_0$ it may take some time until the free precession component $\mathbf{M_0}\hat{\mathbf{e}}_z$ has reached its final value, so before starting any experiments one should wait for about four times T_1[2, 5].

I.B relaxation methods and relaxation times

If no damping effects occurr, the alignment of the spins would be stable. However, experiments show various damping effects with exponential decay.

At first, spin-lattice relaxation has to be considered. The term 'lattice' is used for historical reasons[2] and has no physical implications for this experiment. The idea can be described easily: within an external magnetic field the total magnetization is bigger than zero in equilibrium state but reaches zero for a vanishing magnetic field due to equally occupied energy levels. Thus, there has to be a process that equalizes the occupation numbers after the sample is removed from the magnetic field. This process is called 'spin-lattice relaxation'[3]. The corresponding time constant for the exponential decay is T_1. In some cases, the free precession may continue for a few seconds after the $\mathbf{B_1}$ field is switched off[3].

The second one, the spin-spin relaxation, is a result of the mutual influence of the protons' magnetic fields on all adjacent protons[2]. As the relative phase of the protons changes over time, the total signal decays with the time constant T_2. For protons in water, $T_2 \simeq 3$s[2]. T_2 raises exponentially with increasing temperature[4]. An alternative name for T_2 is the 'transverse relaxation' time[3].

The final one results from imhomogeneous magnetic fields $\mathbf{B}_i$. As $\mathbf{B}_1$ is pulsed and effective for a rather short duration τ only, $\mathbf{B}_0$ has a much higher relevance. The inhomogeneities are given as slightly different field strengths within the sample[2]. The time constant accounting both for the field inhomogeneities and the spin-spin relaxation is called T_2^*. The effects of these inhomogeneities can be compensated by repeated spin echo sequences[4]. The inhomogeneities ΔB can be determined[6] from

$$T_2^* = \frac{\ln 2}{\gamma_I \Delta B} \tag{15}$$

For long pulses, it has to be kept in mind that all relaxation effects affect the spins even during the rotation pulses. Besides the purely method immanent issues, the

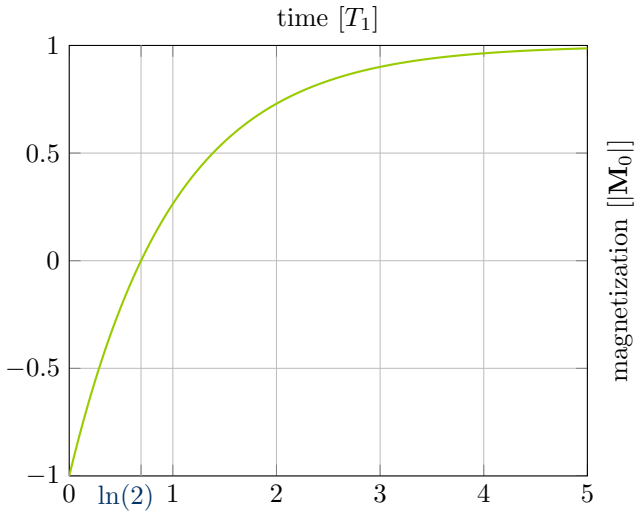

Figure 3. Time dependency of the magnetization response from an inversion recovery pulse at $t = 0$ according to [2]. This describes the longitudinal relaxation[4]. Theoretical values.

strength of the response from the sample may lead to even higher, non-exponential damping[2]. This is the case if the induced field in the receiver coil is strong enough to induce a current within the coil which itself emits a magnetic field. This field can influence the LARMOR frequency and thus alter the measured time dependency of $\mathbf{M}_0$. For protons in water, this induced field is expected to be rather weak[2].

In general, the spin lattice relaxation time T_1 is the longest, as $\mathbf{M_0}\hat{\mathbf{e}}_z$ can only reach its maximal value if the projection of $\mathbf{M_0}$ on the xy-plane is zero, so the transversal relaxation has to be finished. As T_2^* keeps track of additional damping effects in comparison to T_2, T_2^* is shorter than T_2. Therefore, we have[5]

$$T_1 \geq T_2 \geq T_2^* \tag{16}$$

Paramagnetic ions within the sample reduce T_1 and T_2 significantly due to their local magnetic field[3]. Especially the very small electron spin relaxation time of about $3 \cdot 10^{-9}$s results in highly fluctuating fields. Thus, a higher concentration of paramagnetic ions is expected to lead to lower relaxation times. As a rule of thumb, both T_1^{-1} and T_2^{-1} are proportional to the paramagnetic ions' concentration[3]. Additionally, the relaxation times depend both on constant physical properties of the ions as well as on experimental properties like the temperature or pH[3, 7]. When considering BROWNian motion, the temperature dependecy is evident. Throughout the whole experiment the $CuSO_4$ ions are less than 0.36% of the sample, so in case all molecules were fixed, most of the protons would be unaffected by the paramagnetic ions. Therefore, a higher temperature leads to smaller decays. Obviously, changing the pH of the sample changes the probability for every proton to be influenced by a paramagnetic ion.

I.C pulse sequences

Unless otherwise stated, all pulses are issued along $\hat{\mathbf{e}}_\mathbf{x}$.

Each magnetic field pulse $\mathbf{B}_1 \perp \mathbf{B}_0$ with the duration τ and the resonance frequency rotates the vector $\mathbf{M}_0$ through an angle of

$$\alpha = \gamma_I B_1 \tau \tag{17}$$

For $B_1 \gg B_0$, the rotation axis is $\mathbf{B}_1 B_1^{-1}$. For $B_1 \ll B_0$, the rotation axis is $\hat{e}_z$. In all other cases, the rotation axis is given by the effective field resulting from the linear combination of B_1 and B_0. The first case is the usual one[2]. All pulses are being referenced to in terms of α.

The first 'sequence', called 'inversion recovery' is used for determining T_1. It consists of a single π pulse followed by a $\pi/2$ pulse after τ'[5]. The response is given[2] by

$$\mathbf{M}_0(t)\hat{\mathbf{e}}_z = |\mathbf{M}_0(0)| \left[1 - 2\exp\left(-\frac{t}{T_1}\right)\right] \tag{18}$$

In case of repeated experiments with π pulses, the spare time t_p between the successive runs for a relative recovery

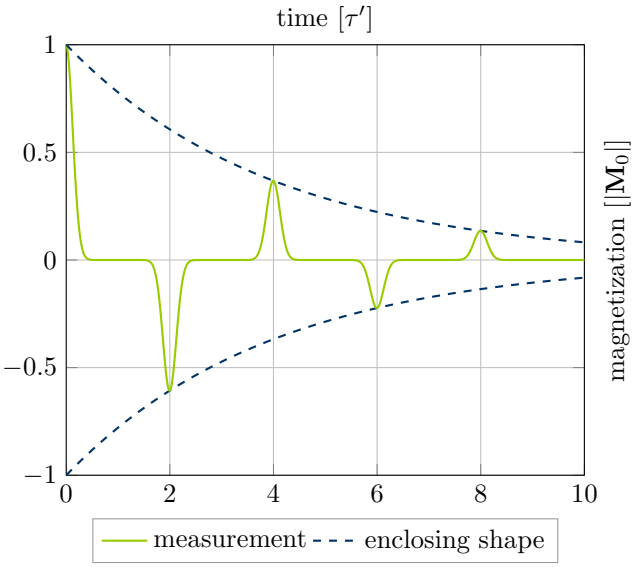

Figure 4. Measurement using the CARR-PURCELL sequence with arbitrary echo shapes but correct amplitudes. The spin echo sequence terminates at $t = 3\tau'$. Theoretical values.

of a is given by

$$\mathbf{M}_0(t_p)\hat{\mathbf{e}}_z = a\mathbf{M}_0(0)\hat{\mathbf{e}}_z \Leftrightarrow t_p = -T_1 \ln\frac{1-a}{2} \tag{19}$$

As shown in Figure 3, T_1 can be directly determined by measuring the zero crossing after $T_1 \ln 2$. However, this is being discouraged from as the results are assumed to be inaccurate[5].

The second sequence 'spin echo' consists of two pulses $\pi/2$, τ', π, τ' with the intermediate pauses τ'[2]. The first $\pi/2$ pulse shifts $\mathbf{M_0}$ from $\hat{\mathbf{e}}_z$ to $\hat{\mathbf{e}}_y$. During the time τ', the spins rotate within the xy-plane. As the rotation frequency depends on the magnetic field, the spins of protons being affected by slightly different magnetic field strengths are being separated. However, the differences in the magnetic field can be assumed[4] to remain static throughout durations of the magnitude of τ'. Thus, the phase difference φ between any of the spins and $\hat{\mathbf{e}}_y$ is linear in τ'. The π pulse between the two pauses reverses the order of the spins within the xy-plane. After the second break, all spins are collinear again, although they are now aligned along $-\hat{\mathbf{e}}_y$.

A slighly modified version is the 'CARR-PURCELL' se-

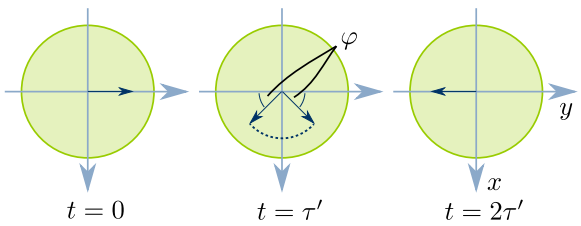

Figure 5. spin-echo sequence[4]

Table II. Overview of measurement methods[5]. Subscript denotes axis.

name	var.	sequence
inversion recovery	T_1	π_x, τ', $\pi_x/2$
spin echo	T_2^*	$\pi_x/2$, τ', π_x
Carr-Purcell	T_2^*	$\pi_x/2$, τ', $(\pi_x, 2\tau')^n$
mod. Carr-Purcell	T_2^*	$\pi_x/2$, τ', $((-1)^n\pi_x, 2\tau')^n$
Meiboom-Gill	T_2^*	$\pi/2$, τ', $(\pi_y, 2\tau')^n$

quence. Basically, the spin echo sequence is repeated over and over until the signal amplitude decreased too far and vanished in the signal noise. As the spins have to be flipped onto the xy-plane only once, the sequence is $\pi/2$, τ', π, $2\tau'$, π, $2\tau'$, ... The major drawback is the error summation. In case the $\pi/2$ pulse is different from the theoretical optimum by a phase β, then the initial projection on $\hat{e}_y$ is smaller but the experimental data itself is unaffected with the exception that the signal might vanish earlier due to the decreased amplitude. But in case the π pulse differs from the optimum in a phase β, the exponential decay gets modulated by a cosine function, so the nth impulse from the Carr-Purcell method is

$$\mathbf{M_0}(t_n)\hat{\mathbf{e}}_y = \cos(n|\beta|)\exp\left(-\frac{t}{T_2^*}\right) \tag{20}$$

One slight adjustment is able to cope with these errors: if the sequence uses alternating π and $-\pi$ pulses, the errors would cancel out. For these measurements, only the peaks with positive amplitude have to taken into account for analysis.

The fourth sequence consists of only one pulse and is used for measuring the free induction decay time T_2^*. One $\pi/2$ pulse shifts $\mathbf{M_0}$ into the xy-plane. Without any external effects, $\mathbf{M_0}$ precesses around $\hat{\mathbf{e}}_z$ while the damping reduces $|\mathbf{M_0}|$.

The fifth sequence is similar to the Carr-Purcell one but all π pulses are issued along $\hat{\mathbf{e}}_\mathbf{y}$ instead of $\hat{\mathbf{e}}_\mathbf{x}$. This 'Meiboom-Gill' method is able to cope with a slight deviation of π pulse length, as well[5]. At first, a $\pi/2$ pulse shifts the magnetization onto $\hat{\mathbf{e}}_y$. The spins start to diverge in the xy-plane and get shifted by the π pulse after τ'. Now all the spins focus again on $\hat{\mathbf{e}}_y$ after τ'. In case the pulse length deviation leads to a phase difference β, the π pulse shifts the magnetization vector to a position slightly off the xy-plane. This error will be corrected by the next π pulse. Again, only every second peak should be considered for the analysis, as they all share the same sign. This method is considered to be advantageous when compared to the extended Carr-Purcell method in terms of experimental effort as all π pulses are positive.

Table II enlists all described pulse sequences and their corresponding observable.

Table III. Adjusted values of the field parameters of the permanent magnet in arbitrary units after adjusting for an optimal field homogeneity. The error was chosen due to inaccuracy in determination of the best shape of the exponential decay and the controller's mechanical clearance.

name	value
X	(0.35 ± 0.05)
Y	(6.72 ± 0.05)
Z	(3.74 ± 0.05)
Z^2	(-6.90 ± 0.05)

II experimental setup

As shown in Figure 1, we used the homogeneous magnetic field with $B = 0.49\,\mathrm{T}$ of a permanent magnet containing a coil. Although a permanent magnet itself does not guarantee a homogeneous field at all, the sample's minor size allows for this assumption. To reach a highly homogeneous static magnetic field over the region of the sample we adjusted the four additional coils nearby the permanent magnet using the corresponding controller. The homogeneity is maximal if the time constant for the exponential time dependency of the free induction decay (FID) is as large as possible. In the beginning, we adjusted the spectrometer with a light mineral oil sample and then continued using a Copper (II) Sulfate solution $CuSO_4$ with different concentrations of 0.05mol, 0.1mol and 0.2mol for the measurements of the relaxation times throughout the experiment. All samples were provided in small cavities with an approximate sample diameter of two millimetres. The settings considered to be optimal in terms of the FID time constant are presented in Table III.

In the second step we determined the resonance frequency of the system. This frequency is expected to match the Larmor frequency in eqn. 9. In order to search for the resonance case, we adjusted the frequency generator's settings and observed the maximum initial intensity $\mathbb{M}(0)$ of the FID. We found $f = 21.048\,\mathrm{MHz}$

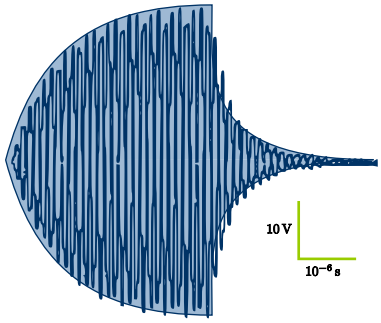

Figure 6. Enclosing shape of a $\pi/2$ pulse (filled) after the adjustment together with the frequency generator output (stroked, thick). The enclosing shape is modulated with $T_L = f^{-1} \simeq 0.048 \cdot 10^{-6}\,\mathrm{s}$. Vectorized oscilloscope output.

whereas the theoretical value is $f_T = 20.863$ for an magnetic field of $B = 0.49\,\mathrm{T}$. As the spectrometer uses the same coil for both the pulses and the signal measurement, a oscillating circuit is necessary to tell signal and response apart. Hence, we had to adjust the eigenfrequency of the inner coil to the resonance frequency of the system by putting a sensor into the samples' position and adapting the corresponding capacities. The oscilloscope showed the pulse shape as recorded by the sensor. The final pulse shape is presented in 6.

In the next step, we adjusted the pulse durations for both the $\pi/2$ and the π pulse. To obtain the duration for $\pi/2$, we observed the FID on the oscilloscope for different pulse lengths. One example is depicted in 7. On a related sidenote, the oscillations on the FID signal result from a setup slightly off resonance. The smaller the modulations, the better the resonance criterion is met.

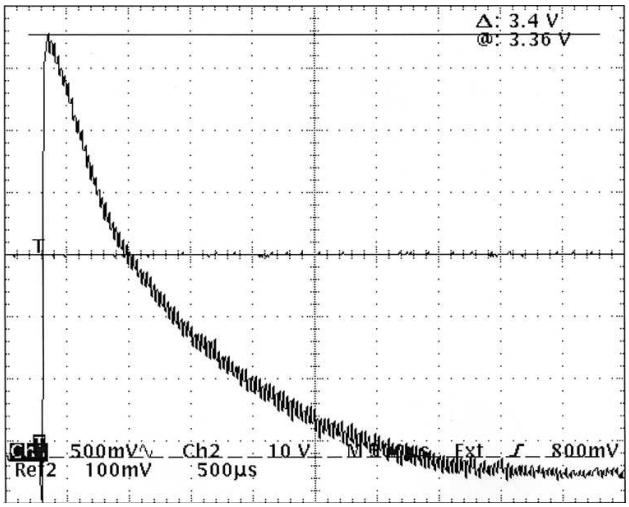

Figure 7. FID with maximal amplitude after a $\pi/2$ pulse of 3.4 ms. Oscilloscope output.

For the $\pi/2$ pulse we found an optimal duration in terms of a maximal FID amplitude of 3.4 ms. Although the angle of rotation depends linearly on the pulse duration according to eqn. (17), we measured the π pulse separately instead of doubling the duration mentioned above. Searching for a minimal FID amplitude, we obtained a π pulse duration of 5.02 ms. As neither pulse duration is supposed to be determined with a high accuracy, the difference of the two times' quotient is obvious but not that important, as only the Carr-Purcell and inversion recovery methods suffers to some extend from inexact π pulses. However, the accuracy of the $\pi/2$ pulses affects mostly the amplitudes but leaves the time contants invariant.

III results

The time between two consecutive pulse sequences has set to at least 480 ms. This is supposed to be by far large enough in order to keep the measurements from interfering.

Table IV. Dependency of T_2^* on the $CuSO_4$ concentration.

concentration [mol/l]	T_2^* [ms]	inhomogeneity [μT]
0.05	(5.11 ± 0.05)	(0.507±0.005)
0.1	(2.43 ± 0.01)	(1.066±0.004)
0.2	(0.99 ± 0.01)	(2.62±0.03)

III.A inhomogeneity

According to the Bloch equations, the time constant T_2^* can be determined from

$$\ln \mathbf{M}_{x,y}(t) = -\frac{t}{T_2^*} + \ln\left[\mathbf{M}_{x,y}(t_0)\right] \tag{21}$$

To calculate the influence of the inhomogeneity of the magnetic field on the relaxation time we analyzed the intensity of the FID signal after a single $\pi/2$ pulse for different values of τ. From the slope of 21 T_2^* can be obtained. The results for three different concentrations are given in Table IV.

The three values of T_2^* should be equal, as T_2^* only depends on the inhomogeneity of the magnetic field but does not depend on the $CuSO_4$ concentration in the sample. Nevertheless, the measured values are significantly different. The measurement of the peaks' intensities of the FID happened to be very precise, hence the error arises mainly from the variation of the measured values from the linear fit caused by a systematic error. This is a result of the fact, that we solved the Bloch equation under the assumption that T_2^* is large compared to T_2 but during the measurement it turned out that they are of same order so we measured a combination of both relaxation times. For the calculation of ΔB according to eqn. (15) we used the average of T_2^* and got

$$\Delta B = (0.91 \pm 0.05)\,\mu\mathrm{T}$$

III.B spin-spin relaxation time T_2

The spin-spin relaxation time T_2 can be measured by applying several methods discussed in the introduction, namely spin-echo Carr-Purcell (CP) and Meiboom-Gill (MG). We performed the measurement refering to CP via an initial π pulse followed by $N \geq 10$ $\pi/2$ pulses. Surprisingly the second and fourth peak are methodically too low compared to the expectations build by the surrounding peaks and do not fit into the exponential decay so we decided to ignore them for the calculation of the relaxation times.

We plotted the peaks' logarithmic intensity over the time as multiples of τ. From the slope of the linear fit we could obtain the values for T_2. as shown in Figure 9.

We followed the same procedure for MG and spin-echo to obtain the values of T_2 of those methods. The peaks

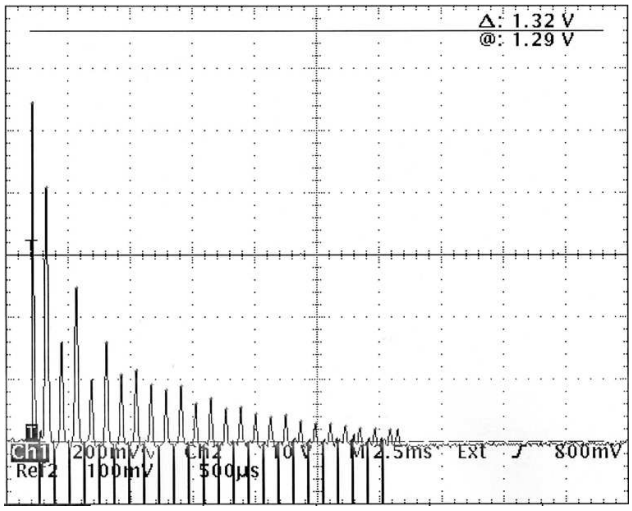

Figure 8. Intensity of $\mathbf{M}_{x,y}$ versus delay times τ via CP method of 0.05mol $CuSO_4$

.

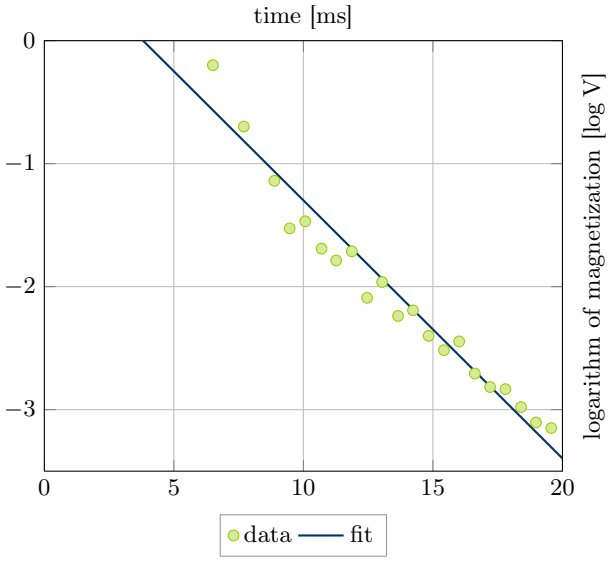

Figure 9. TODO Linear regression fit for CP method of 0.05mol $CuSO_4$ to calculate T_2. We find $T_2 = (4.77 \pm 0.11)$ms

itself are again very accurate so the error of T_2 mainly arises from the systematic error as for CP because we found the second peak to be significantly too short for an exponential decay. Hence we neglected it for the calculation of T_2. The spin-echo method just consists of two peaks so the relaxation time for that method might be significantly too long as the slope of the line between the two peaks might be too steep. The results of all methods are presented in Table V.

Figure 10 shows the dependency of T_i on the $CuSO_4$ concentration. For both times, the function

$$g(x) = \frac{c}{x} + d \tag{22}$$

Table V. T_2 for different concentrations of the $CuSO_4$ samples measured with spin-echo (SE), the Carr-Purcell method (CP) and the Meiboom-Gill method (MG).

	0.05mol	0.1mol	0.2mol
SE	(5.61 ± 0.01)	(0.53 ± 0.90)	–
CP	(4.77 ± 0.11)	(3.03 ± 0.09)	(1.36 ± 0.05)
MG	(8.67 ± 0.17)	(4.93 ± 0.22)	(1.41 ± 0.08)

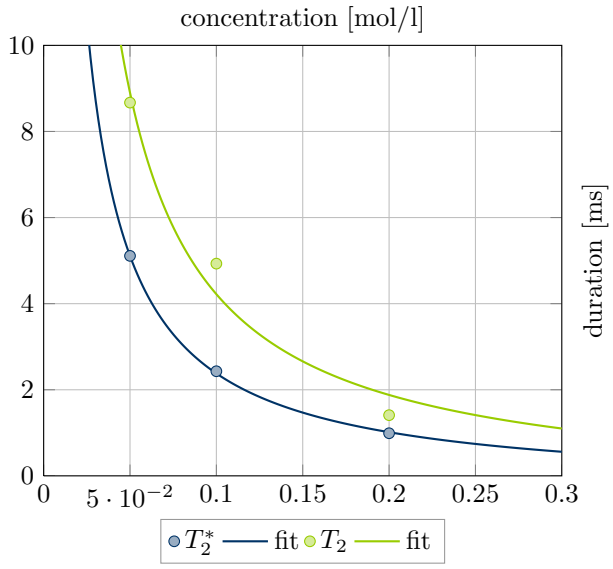

Figure 10. Dependency of T_i on the $CuSO_4$ concentration.

for the concentration x has been used as basis for the fit. For T_2^*, the resulting parameters are

$$c = 0.273 \frac{\text{ms} \cdot \text{l}}{\text{mol}} \qquad d = -0.35\text{ms}$$

and for T_2, we get

$$c = 0.468 \frac{\text{ms} \cdot \text{l}}{\text{mol}} \qquad d = -0.46\text{ms}$$

III.C spin-lattice relaxation time T_1

T_1 has been measured using the inversion recovery pulse sequence. Firstly, a π pulse flips the sign of $\mathbf{M}\hat{\mathbf{e}}_z$. The following $\pi/2$ pulse rotates $\mathbf{M}$ into the xy-plane and thus makes the former z-component detectable. By changing the duration of the break τ between the two pulses, we can investigate the expected exponential decrease of the amplitude of $\mathbf{M}\hat{\mathbf{e}}_z(t)$. Fitting the parameters a and b with the measured data for the 0.05 molar $CuSO_4$ solution from Figure 11

$$f(t) = a \cdot \left[1 - 2\exp(-b^2 t)\right] \tag{23}$$

gives

$$a = (1.102 \pm 0.025)\,\text{V}$$

$$b = (-0.1939 \pm 0.0030)\,\mathrm{s}^{-1/2}$$

The resulting fit is visualized in Figure 11, as well.

The corresponding time constant T_1 can be determined in two ways: either the zero crossing of the magnetization has to be observed or the fit parameter b has to be interpreted. The zero crossing is considered to be rather unreliable, as performing measurements near the zero value was difficult. On top, a linear fit of the data points before the zero crossing results in a different zero crossing as fitting the data points right after the expected position. Thus, we deciced to let these two fits determine the error for the zero crossing method. This way, we get

$$T_1 = (24 \pm 4)\,\mathrm{ms}$$

Using

$$T_1 = \frac{1}{b^2} \tag{24}$$

$$\Delta T_1 = \left|\frac{\partial T_1}{\partial b}\Delta b\right| = 2\frac{\Delta b}{b^3} \tag{25}$$

the result is

$$T_1 = (26.598 \pm 0.003)\,\mathrm{ms}$$

Both values are statistically identical.

IV discussion

In the NMR experiment we used different techniques to measure relaxation times and confirm theoretical expectations. We prepared our system with different samples and generated pulses to measure the time dependence of the magnetization using various methods.

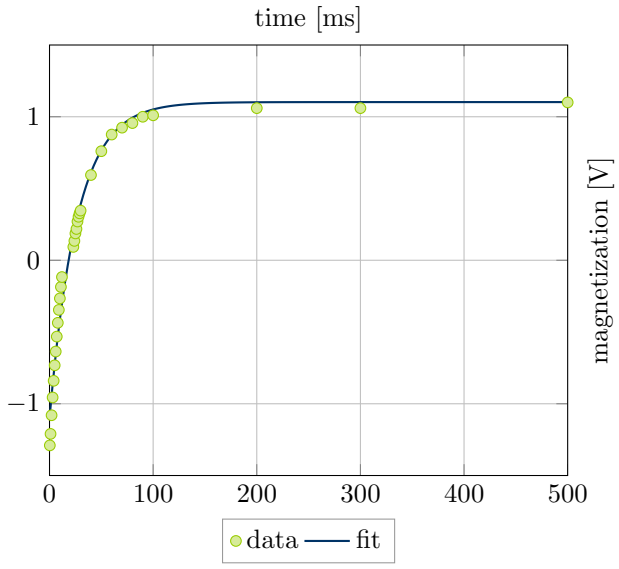

Figure 11. Data measured for T_1 by inversion recovery for the molar $CuSO_4$ solution and a fit.

First of all, we measured the spin-lattice relaxation time T_1 using the inversion recovery method. We obtained $T_1 = (24 \pm 4)\,\mathrm{ms}$ by the zero crossing of the magnetization and $T_1 = (26.598 \pm 0.003)\,\mathrm{ms}$ from the fit. In general, the value of T_1 extracted from the fit is more accurate as the zero crossing strongly depends on rather accurate values for $\mathbf{M}_z \simeq 0$. However, the data near the zero crossing was of the same order of magnitude as the background noise.

The second method seems to suffer from a systematic error as the magnetization does not return to its full initial value but remains about 15 percent smaller instead. However, the asymptotical behavior matches the fitted curve. Therefore, it seems reasonable to blame the high initial value for the difference. Additionally, just around the zero crossing the exponential dependency seems to be broken as the part after the zero crossing seems to be shifted to bigger times.

In the next step, we analyzed the inhomogeneity of the applied static magnetic field for different concentrations of $CuSO_4$ samples. Theory predicts that the relaxation time is just dependent on the inhomogeneity of the field but not on the paramagnetic ions' concentration. Hence, we measured the characteristic relaxation time T_2^* which was expected to be in the region of several ms. We can confirm that expectation but our measurements have also shown a concentration dependence. The higher the concentration of $CuSO_4$ ions, the smaller the relaxation time. This violates our theoretical expectations for T_2^* but matches the expectations for T_2. Although the measurement ifself turned out to be very accurate, the intensity of the peaks did not fit the characteristic exponential decay very well. There was some systematic error because we can observed that the decay happens faster than it should by theory. The reason for this could be a non-linear inhomogeneity of the field or the off resonance setting which leads to a faster decay than theoretically expected. We found that inhomogeneity of the magnetic field is $\Delta B = (0.91 \pm 0.05)\,\mu\mathrm{T}$.

Up next, we investigated the real spin-spin relaxation time T_2 by using three different methods namely spin-echo, Carr-Purcell and Meiboom-Gill. From theory, we expect that the relaxation time decreases with increasing $CuSO_4$ concentration. In general, we expect CP to be less accurate than SE or MG. In addition to that, we observed that the second intensity peak always was significantly too short.

The CP method is very dependend on the exact duration of the π pulse which itself requires an accurately adjusted resonance frequency of the system. Hence, we expect the MG method to provide the most precise values for T_2 because it is more resistent to errors concerning the π pulse. An error for the π pulse results in a apparently faster decay of the signal which means T_2 will decrease. The results shown in Figure V. Our measurement confirms these expectations, as the results of the MG method shows the best linear dependency between relaxation time and concentration of $CuSO_4$ ions as sug-

gested by [3].

Furthermore, according to theory, the T_2^* relaxation times should be higher than the corresponding T_2 values but we found them to be almost equal and T_2^* shows the same concentration dependency as T_2 which is contradicting the theory.

All in all, we could confirm most the general statements listed in the theoretical section. The spin-lattice relaxation time T_1 is significantly higher than the spin-spin relaxation times T_2 and T_2^*. The expected dependence between spin-spin relaxation time and concentration of $CuSO_4$ ions could also be confirmed. Nevertheless, we observed some systematic errors during the measurement. The relaxation times decreased too fast, which may result from a suboptimal π pulse. The prints of the oscilloscope signal showed sharp intensity peaks but also fluctuated a lot. Hence, as we always measured average values, we may have estimated the errors in the peaks' intensity too small, which might be one reason for the error in decay rates.

[1] W. Demtröder, *Experimentalphysik 3* (Springer, 2010).

[2] R. Freeman, *Spin Choreography–Basic steps in high resolution NMR* (Oxford University Press, 1998).

[3] A. Carrington, *Introduction to Magnetic Resonance* (Harper and Row, 1969).

[4] B. Cowan, *Nuclear Magnetic Resonance and Relaxation* (Cambridge University Press, 1997).

[5] E. B. T. Farrar, *Pulse and Fourier Transform NMR–Introduction to Theory and Methods* (Academic Press, 1971).

[6] *Script 'Pulsed Nuclear Magnetic Resonance'* (FU Berlin).

[7] S. Meiboom, J. Chem. Phys. **34**, 375 (1961).